Journal of Mines, Metals and Fuels, *71(12B): 131-138; 2023. DOI: 10.18311/jmmf/2023/45540*

Print ISSN : 0022-2755

Journal of Mines, Metals and Fuels

Contents available at: *www.informaticsjournals.com/index.php/jmmf*

A Review of the Effects of Injection Strategy and Combustion Chamber Geometry Modification and a Single - Cylinder Diesel Engine

Sudipta Nath[1,2], Ranjan Kumar[2]*, Shahanwaz Khan[3] and Somnath Das[1]

[1]*Department of Mechanical Engineering, Swami Vivekananda Institute of Science and Technology, Kolkata - 700145, West Bengal, India*

[2]*Department of Mechanical Engineering, Swami Vivekananda University, Kolkata - 700121, West Bengal, India; ranjansinha.k@gmail.com*

[3]*Department of Mechanical Engineering, Aliah University, Kolkata - 700156, West Bengal, India*

Abstract

Diesel engines are extensively utilized in India's stationary power generation and agricultural pumping applications. Recent stringent government emission regulations necessitated modifications to existing engines. This study investigates a stationary, direct-injection, single-cylinder, 10 HP Diesel engine that initially did not comply with these norms. The original engine, featuring a hemispherical piston bowl and an injector with a finite sac volume, was modified to include a re-entrant combustion chamber and a sac-less injector. These modifications led to significant changes in emission levels. The study also highlights the critical influence of piston bowl shape on engine performance and emissions. Experimental and numerical analyses, including the use of multi-swirl piston bowls (MSB) and double-swirl piston bowls (DSB), revealed that these designs enhance in-cylinder swirl and turbulence, thereby improving the combustion process and reducing soot emissions by up to 81%. However, these modifications also increase NOx emissions due to elevated in-cylinder temperatures. Optimizing injection parameters could mitigate NOx emissions while maintaining engine performance. Thus, the proposed combustion chamber geometries and optimized injection strategies offer a promising approach to achieving compliance with stringent emission standards.

Keywords: *CFD, Diesel Engine, Fuels, Performance of Emission*

1.0 Introduction

Diesel engines are extensively used for non-road and transportation purposes due to their superior thermal efficiency, reliability, and fuel economy. Despite ongoing advancements in diesel engine technology aimed at increasing efficiency and reducing emissions, the agricultural and maritime sectors continue to rely heavily on diesel engines where fuel economy remains a critical parameter. Compared to gasoline engines, diesel engines emit lower levels of CO and HC but produce higher levels of PM and NOx, which are known to have carcinogenic effects. Consequently, various approaches have been developed to mitigate diesel engine emissions, including the use of alternative fuels, combustion chamber improvements, high-pressure injection systems, turbocharging, intercooling, Exhaust Gas Recirculation (EGR), particle filters, and Selective Catalytic Reduction (SCR)[1-4].

*Author for correspondence

Among these methods, optimizing the combustion chamber and fluid motion within the engine is one of the most effective ways to reduce emissions. The primary goal of enhancing the combustion chamber is to maximize combustion efficiency while minimizing exhaust emissions. Modelling plays a crucial role in developing and optimizing internal combustion engines by simulating thermodynamics, fluid flow, heat transfer, combustion, and emission formation events. As computational capabilities improve, the ability to solve complex equations and deepen our understanding of these phenomena advances, leading to more accurate and efficient engine models[5-7].

Numerous experimental and numerical studies have investigated diesel engine performance and emission characteristics. Hentschel and Schindler demonstrated the analysis of in-cylinder flow, fuel injection, and combustion using advanced techniques like QS laser and Laser Doppler Anemometer (LDA)[8], highlighting the importance of vortex interaction, spray formation, and combustion in engine development. Payri *et al.* designed various piston bowls for a four-valve, direct-injection diesel engine and validated their CFD simulations with experimental results, showing the critical influence of piston configurations on flow characteristics near TDC. Yılmaz *et al.* examined the effects of compression ratio, injection timing, and cone angle on HCCI engine performance, using high-pressure fuel spray and air motion analyses[9,10].

Benajes *et al.*[11-13] studied piston bowl geometry in RCCI engines, finding that shallow bowl geometries with smaller surface areas improved gross work at low load conditions. Kakaee *et al.*[14-17] explored different piston bowl geometries and their effects on combustion characteristics at various engine speeds, revealing significant impacts on NOx emissions and the importance of bowl profile at high speeds. Li *et al.*[18-21] proposed a new multi-swirl bowl design, which demonstrated lower BSFC and soot emissions, attributing these improvements to enhanced fuel-air mixing. Additional studies by Li *et al.* on lateral swirl combustion chambers indicated improved air-fuel mixing and reduced soot emissions due to the guiding effects of the chamber geometry.

Stringent emission norms imposed globally have necessitated further exploration of combustion chamber geometries. This study focuses on the effect of re-entrancy in the combustion chamber geometry of a single-cylinder, 948 CC, 10 HP diesel engine[22]. The objective is to explore the potential of re-entrant chambers to lower emissions while maintaining engine performance. In diesel engines, the air in the cylinder is transferred into the combustion chamber at the end of compression, meaning changes in chamber geometry significantly affect the flow field during critical events like spray and combustion. Parameters such as swirl, squish, and turbulence are crucial in designing diesel engines, with swirl motion being particularly significant for combustion efficiency.

Previous studies have shown that re-entrant chambers can increase NOx but reduce smoke emissions. Re-entrant chambers also enhance in-cylinder velocities and swirl, leading to improved turbulence and combustion characteristics. However, most research on re-entrant chambers has focused on large engines, with limited studies on medium and small engines. This study addresses this gap by investigating the introduction of re-entrancy to the combustion chamber of a single-cylinder, 10 HP, 948 CC engine. Both experimental and computational analyses are conducted to assess the impact of re-entrant chamber geometry on engine performance and emissions, providing insights into optimizing small diesel engines for compliance with stringent emission standards[22].

2.0 Experimental Setup and Procedure

A four-stroke, single-cylinder, direct-injection diesel engine was used for the trials. Table 1 provides a brief description of the test engine's features. The engine has a displacement volume of 0.51 L with a bore and stroke of 85 and 90 mm, respectively. Figure 1 displays an image of the experimental setup, and Figure 2 provides a schematic diagram of the experimental arrangement. The test engine, dynamometer, exhaust gas analysis system, and in-cylinder pressure monitoring system make up the test setup. The test engine's operating temperature was maintained throughout by the cooling tower. An AC dynamometer with a maximum power of 53 kW, a maximum torque of 120 Nm, and a maximum speed of 8000 rpm was installed in the test engine. The dynamometer control software (MpiCON) was used to record data and control the engine. Using a Rheonik

RHM 03 Coriolis flow metre, fuel mass was determined with an accuracy of 0.1%.

Performance and emission tests with measured load and emission data are part of the experimental research done on this engine. The tests were carried out at 10%, 25%, 50%, 75%, and 100% of the maximum load, according to the given drive cycle. The engine's static injection timing is 26° CA BTDC. To make sure that the experimental conditions could be repeated, the engine inlet pressure was kept at 100 kPa.

Table 1. Characteristics of test engine

Engine Type	Single cylinder, naturally aspirated, four-stroke, and direct injection
Total displacement	510 cm^3
Bore	85 mm
Stroke	90 mm
Connecting rod length	144.5 mm
Piston pin offset	0.0 mm
Compression ratio	17.5
Maximum power	12 HP
Maximum torque	32 Nm
Bore/Stroke	0.9444
Injection type	Mechanical, 200 bar
Cooling	Water

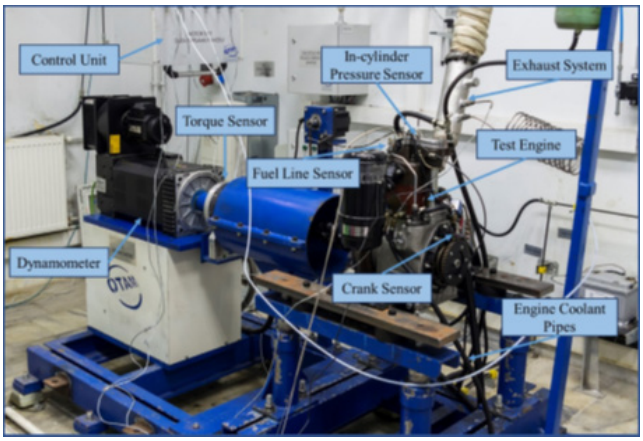


Figure 1. The picture of the experimental setup.

For a specific cycle at each load in these studies, the injector needle lift, injection line pressure, and cylinder pressure were recorded. Once the engine had warmed up sufficiently, emission data were acquired for unburned hydrocarbons (HC), carbon monoxide (CO), particulate matter (PM), and NO_X. Table 2 represents the results output of performance and emission tests.

According to emission regulations, various weighting factors are assigned to different loads to determine the final emission levels of an engine. The calculated emission levels, based on these weighting factors, must fall within the specified limits. Table 3 provides the weighting factors designated by the Central Pollution Control Board (CPCB) as part of the drive cycle.

The hemispherical bowl design results in a portion of the air being inaccessible for combustion, as illustrated in Figure 2. This inefficiency in combustion leads to

Table 2. Results obtained from performance and emission tests.

% of Max Load	Fuel cons. (g/hr)	Power (kW)	Emissions (g/hr)		
			HC	CO	NO_X
10	620	0.76	9.66	20.00	23.51
25	800	1.89	9.82	18.68	34.85
50	1120	3.75	9.90	15.65	48.59
75	1460	5.56	10.13	13.67	63.34
100	1850	7.30	11.36	58.71	75.45

Table 3. Weighting factors specified by CPCB norms.

% of Max. Load	10	25	50	75	100
Weighting factor (Wf)	0.1	0.3	0.3	0.25	0.05

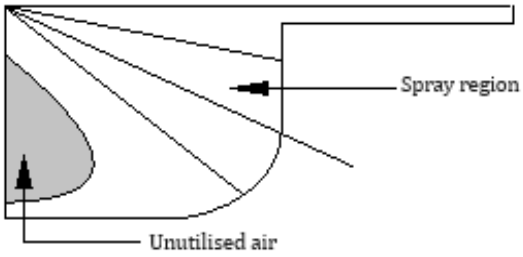


Figure 2. Engine geometry before modifications.

increased HC emissions. Furthermore, the lack of available air in the spray region can result in unburnt fuel, which subsequently transforms into Particulate Matter (PM).

Based on these observations, several modifications were proposed for the engine. The combustion chamber was redesigned as a re-entrant chamber, and the injector was replaced with a sac-less injector featuring 0.26 mm holes, compared to the previous 0.28 mm holes. It was anticipated that the re-entrant design would enhance mixing, thereby reducing both HC and NOx emissions by minimizing the premixed phase of combustion. The sac-less injector significantly reduces HC emissions, while the smaller injector holes facilitate quicker spray breakup and fuel evaporation, potentially decreasing the ignition delay. Although re-entrant chambers can increase NOx emissions due to improved mixing and combustion, the injection timing was delayed by 4° CA to mitigate this effect. The compression ratio remained unchanged by ensuring the volumes of the two bowls were equivalent.

The proposed modifications were implemented, and tests were conducted on the modified engine. Table 4 presents the emission values of the modified engine and compares them with the emission levels of the original configuration.

The proposed modifications were implemented, and subsequent tests were conducted on the modified engine. Table 4 presents the post-modification emission values and compares them to those of the original configuration. Notably, HC emissions were reduced by 66.8%, achieving a satisfactory margin relative to CPCB norms, largely due to the injector replacement. CO emissions increased slightly by 4.12%, while delayed injection resulted in a 30% reduction in NOx emissions. Improved mixing and combustion reduced PM by 64%.

Overall, the modifications yielded favourable results, although the emission levels remained above the specified norms. To ensure compliance, a margin of 15% to 20% beyond the minimum requirements is necessary. Given the expense and time-consuming nature of a trial-and-error experimental approach for further emission reductions, it was decided to utilize numerical simulations. Thus, 3-D Computational Fluid Dynamics (CFD) simulations of the

Table 4. Comparison of emission data of modified engine with unmodified engine and CPCB norms.

Pollutant	**Unmodified engine (g/kW/hr)**	**Modified engine (g/kW/hr)**	**Govt. norms (g/kW/hr)**	**Margin (%)**
HC	2.83	0.94	1.3	27.32
CO	5.58	5.81	3.5	-65.94
NOX	13.34	9.33	9.2	-1.40
PM	1.399	0.504	0.3	-68.00

in-cylinder processes were undertaken to provide insights and future guidelines for additional modifications to achieve the desired emission levels.

3.0 Computational Investigation

As previously mentioned, numerical simulations are invaluable for estimating the complete 3-D flow structure, swirl-squish interaction, and turbulence distribution within the cylinder. CFD also elucidates the interactions between fuel and air and identifies regions of pollutant formation. This knowledge can inform further engine modifications to reduce emission levels.

CFD simulations were conducted for the suction, compression, and expansion strokes of both engine configurations (pre- and post-modification). The specialized IC engine simulation software AVL-FIRE was employed for this purpose. This features an automatic hybrid mesh generator that creates a hexahedral-dominated hybrid mesh. Following mesh generation, the moving mesh generator prepares the mesh with moving boundaries required for analysis. The solver initiates the solution after specifying various boundary conditions, initial conditions, models, and model constants. The models used in the current study are listed below:

1. Flow – The compressible Navier-Stokes equations were solved using the SIMPLE algorithm.

2. Turbulence – The k-ε model, combined with the wall function method, was employed.

On the other hand, the numerical simulations were conducted using the commercial CFD code, Converge CFD. This software solves the Reynolds-averaged Navier-Stokes (RANS) equations, including turbulence models, within a multi-dimensional domain. A modified cut-cell Cartesian grid method was employed for meshing, with the domain being re-meshed at each time step to accommodate moving boundaries. Adaptive Mesh Refinement (AMR) was utilized to refine the grid based on dynamic conditions such as temperature or velocity.

The dynamics of fluid flow are governed by equations that ensure conservation of energy, momentum, and mass. Additional equations account for turbulence as well as the transport of passive scalar and species. For accurate, straightforward, and efficient solution, the Renormalization Group (RNG) k-ε model was chosen to calculate turbulent flow within the cylinder. To model the combustion process within the cylinder, the Extend Coherent Flame Model, 3-Zone (ECFM-3Z Model) was employed. This model categorizes the combustion region into three zones: unmixed, mixed air and fuel, and unmixed fuel. Flame propagation occurs from the burned gas to the unburned gas section, considering self-ignition, premixed flame, and diffusion flame combustion modes. The ECFM-3Z model accurately estimates the mixing process, auto-ignition delay, and post-oxidation of fuel.

Engine models with various bowl geometries were designed for parametric simulations involving different spray angles and injection pressures. Following the arrangement of these geometries, computational meshing was necessary for the CFD model. The orthogonal hexahedral mesh was automatically generated based on user-defined control parameters within the CFD code. During the simulation, the grid dynamically adjusts according to piston and valve movements at each time step. The CFD code employs the Adaptive Mesh Refinement (AMR) technique to control cell size based on velocity, temperature, species, passive scalars, and boundaries to ensure convergence. In this study, the maximum embedding level for temperature and velocity was set to three. Fixed refinement was applied to the spray region, liner, cylinder head, and piston walls.

For fuel, n-heptane was used to simulate diesel. Droplet parcels were introduced into the cylinder at specific rates, with each parcel representing a set of identical droplets. These droplets undergo various processes from injection to vaporization. Interface forces acting on the droplets during their relative motion may cause instability, addressed using a breakup model. Among the various models available, the KH-RT model was chosen due to its widespread use in similar cases.

An evaporation model was used to describe changes in the discrete phase based on the droplet's boiling or critical temperature. The Frossling correlation was applied to account for convection effects, assuming spherical symmetry in the diffusion around the droplet surface. Models that fully solve the flow around the droplet increase accuracy but significantly raise CPU time. Therefore, the Frossling model was selected to predict the spray evaporation process, determining the rate of change in droplet size based on the Sherwood number, laminar mass diffusivity of fuel vapor, and mass transfer number.

4.0 Results and Discussion

Simulations were conducted at a constant engine speed of 2800 RPM and under full load conditions. Following validation and mesh independence studies, the model was solved for three cycles. Initial conditions, as well as swirl and tumble values from -100° bTDC of the last solved cycle, were used to start subsequent cases at this crank angle. The initial in-cylinder mixture was assumed to be fully homogeneous and uniform, with a swirl profile of 3.11 and a swirl ratio of 0.8273. At the start of the simulation, the air temperature and in-cylinder pressure were set to 389.9 K and 170.6 kPa, respectively. Initial turbulent kinetic energy and dissipation rates, derived from a full engine three-cycle simulation, were 29.997 m^2/s^2 and 13545.6 m^2/s^3, respectively. The wall temperatures for the piston, liner, head, intake valve, and exhaust valve were set to 525 K, 400 K, 450 K, 550 K, and 450 K, respectively.

Due to the asymmetrical combustion chamber of the test engine, it could not be modelled as a sector, resulting in increased solution time. In-cylinder pressure values for BB, RB, DSB, and MSB were compared at spray angles of 120°, 140°, and 150° under full-load operation, as shown in Figure 2, to understand the combustion process. Results indicated that in-cylinder pressures for MSB and DSB were higher than those for BB and RB, likely due to better fuel mixing and faster evaporation associated with their bowl shapes. MSB and DSB showed similar trends, with MSB reaching slightly higher peak pressures at a spray angle of 140°, while DSB achieved higher peak pressures at a spray angle of 150°. BB generally exhibited the lowest in-cylinder pressures. Given that in-cylinder pressures are directly related to engine power, MSB and DSB configurations are expected to yield higher power output.

On the other hand, the simulations indicate significant potential for emission reduction through optimization of combustion chamber geometry. Considering this and evaluating designs from the literature, a third geometry with increased re-entrancy and no central projection is proposed. The bowl shape is depicted in Figure 3, with its volume chosen to match that of the baseline engine, thereby maintaining the same compression ratio. Based on previous findings showing that end-of-suction flow field and TKE distribution are not dependent on bowl geometry, calculations for the proposed geometry begin at the end of suction and continue through to the end of the expansion stroke.

Figure 4 illustrates the swirl variation with crank angle during the compression and expansion strokes for the proposed engine, comparing these values with those

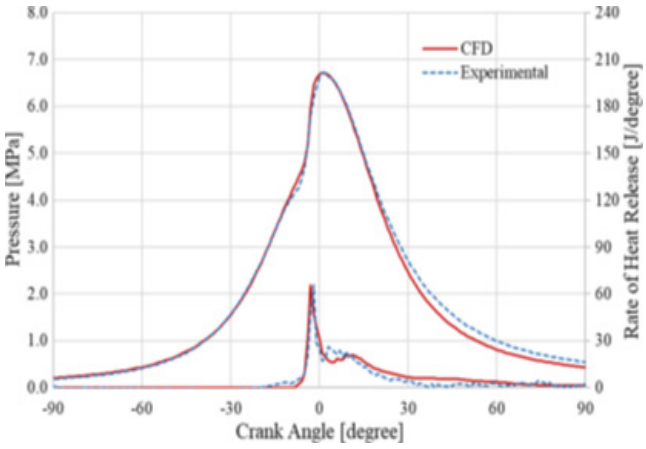


Figure 3. Validation of the CFD model with experimental result.

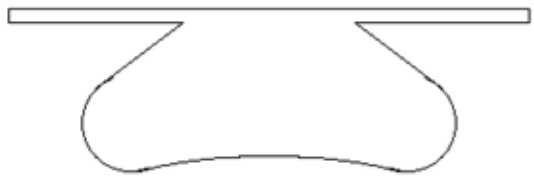


Figure 4. Proposed geometry to improve swirl and TKE levels.

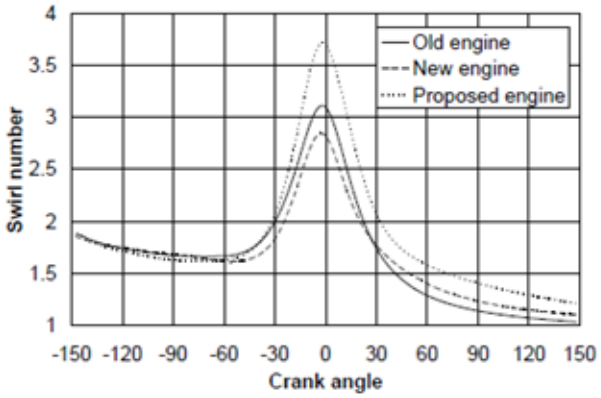


Figure 5. Variation of swirl number with crank angle during the closed valve part of the cycle.

of the two previous geometries. The swirl intensification in the proposed engine is significantly higher, with peak values approximately 20% greater than those of the original engine. Figure 5 displays the variation of average TKE across all three geometries, revealing substantial turbulence intensification near TDC in the proposed design.

5.0 Conclusion

Computational investigations of in-cylinder fluid dynamics in a 12 HP, single-cylinder DI Diesel Engine have been conducted alongside experimental emission data. Emissions of NOX, PM, HC, and CO were measured under various loads for both the original engine configuration and a modified version featuring a re-entrant chamber and sac-less injector. The modified engine exhibited significantly lower emission levels compared to the original.

To understand the impact of re-entrancy on emission reduction, detailed three-dimensional CFD simulations of in-cylinder processes were performed. It was observed that the swirl and TKE levels in the modified engine were consistently lower than in the original engine. The re-entrant design's effect appears to be counteracted by the large central projection, leading to increased skin friction and reduced squish-induced TKE. Therefore, the emission reductions are primarily attributed to changes in injector characteristics. A third combustion chamber design was proposed and subjected to detailed numerical simulations. This new design demonstrated significantly higher swirl and TKE values compared to the baseline configuration, indicating substantial potential for further emission reductions.

6.0 References

1. Sener S, Yangaz MU, Gul MZ. Effects of injection strategy and combustion chamber modification on a single-cylinder diesel engine. Fuel. 2020; 266:117-22. https://doi.org/10.1016/j.fuel.2020.117122
2. O'Driscoll R, Stettler MEJ, Molden N, Oxley T, ApSimon HM. Real-world CO_2 and NOx emissions from 149 Euro 5 and 6 diesel, gasoline and hybrid passenger cars. Sci Total Environ. 2018. https://doi.org/10.1016/j.scitotenv.2017.11.271. PMid:29186703
3. Boccardo G, Millo F, Piano A, Arnone L, Manelli S, Fagg S, *et al.* Experimental investigation on a 3000-bar fuel injection system for a SCR-free non-road diesel engine. Fuel. 2019. https://doi.org/10.1016/j.fuel.2019.01.122.
4. Hanson R, Curran S, Wagner R, Kokjohn S, Splitter D, Reitz RD. Piston bowl optimization for RCCI combustion in a light-duty multi-cylinder engine. SAE Int J Engines. 2012. https://doi.org/10.4271/2012-01-0380
5. Chen Y, Lv L. The multi-objective optimization of combustion chamber of DI diesel engine by NLPQL algorithm. Appl Therm Eng. 2014. https://doi.org/10.1016/j.applthermaleng.2014.09.028
6. Lee S, Jeon J, Park S. Optimization of combustion chamber geometry and operating conditions for compression ignition engine fueled with pre-blended gasoline-diesel fuel. Energy Convers Manag. 2016. https://doi.org/10.1016/j.enconman.2016.08.046
7. Kim HJ, Park SH. Optimization study on exhaust emissions and fuel consumption in dimethyl ether fueled diesel engine. Fuel. 2016. https://doi.org/10.1016/j.fuel.2016.06.001
8. Broatch A, Olmeda P, Margot X, Escalona J. New approach to study the heat transfer in internal combustion engines by 3D modelling. Int J Therm Sci. 2019; 138:405-15. https://doi.org/10.1016/j.ijthermalsci.2019.01.006
9. Rajak U, Nashine P, Verma TN, Pugazhendhi A. Performance, combustion and emission analysis of microalgae Spirulina in a common rail direct injection diesel engine. Fuel. 2019; 255:115855. https://doi.org/10.1016/j.fuel.2019.115855
10. Shu J, Fu J, Liu J, Ma Y, Wang S, Deng B, *et al.* Effects of injector spray angle on combustion and emissions characteristics of a Natural Gas (NG)-diesel dual fuel engine based on CFD coupled with a reduced chemical kinetic model. Appl Energy. 2019; 233-234:182-95. https://doi.org/10.1016/j.apenergy.2018.10.040
11. Hentschel W, Schindler KP. Flow, spray and combustion analysis by laser techniques in the combustion chamber of a direct-injection diesel engine. Opt Lasers Eng. 1996. https://doi.org/10.1016/0143-8166(95)00091-7
12. Payri F, Benajes J, Margot X, Gil A. CFD modelling of the in-cylinder flow in direct injection diesel engines. Comput Fluids. 2004. https://doi.org/10.1016/j.compfluid.2003.09.003
13. Yilmaz M, Koten H, Zafer Gul M. Effects of the injection parameters and compression ratio on the emissions of a heavy-duty diesel engine. Int J Veh Des. 2012. https://doi.org/10.1504/IJVD.2012.048691

14. Benajes J, Garcia A, Pastor JM, Monsalve-Serrano J. Effects of piston bowl geometry on reactivity-controlled compression ignition heat transfer and combustion losses at different engine loads. Energy. 2016. https://doi.org/10.1016/j.energy.2016.01.014
15. Kakaee AH, Nasiri-Toosi A, Partovi B, Paykani A. Effects of piston bowl geometry on combustion and emissions characteristics of a natural gas/diesel RCCI engine. Appl Therm Eng. 2016. https://doi.org/10.1016/j.applthermaleng.2016.03.162
16. Li X, Qiao Z, Su L, Li X, Liu F. The combustion and emission characteristics of a multi-swirl combustion system in a DI diesel engine. Appl Therm Eng. 2017; 115:1203-12. https://doi.org/10.1016/j.applthermaleng.2016.10.028
17. Li XR, Yang W, Su LW, Liu FS. Mixing and combustion mechanisms within Lateral Swirl Combustion System (LSCS) in a DI diesel engine. Appl Therm Eng. 2017. https://doi.org/10.1016/j.applthermaleng.2017.05.089
18. Jafari M, Parhizkar MJ, Amani E, Naderan H. Inclusion of entropy generation minimization in multi-objective CFD optimization of diesel engines. Energy. 2016; 114:526-41. https://doi.org/10.1016/j.energy.2016.08.026
19. Mauro S, Şener R, Gul MZ, Lanzafame R, Messina M, Brusca S. Internal combustion engine heat release calculation using single-zone and CFD 3D numerical models. Int J Energy Environ Eng. 2018; 9:215-26. https://doi.org/10.1007/s40095-018-0265-9
20. Şener R, Ozdemir MR, Yangaz MU. Influence of piston bowl geometry on combustion and emission characteristics. Proc Inst Mech Eng Part A J Power Energy. 2019; 233:576-87. https://doi.org/10.1177/0957650919854637
21. XiangRong L, WeiHua Z, LiWang S, FuShui L. Research on energy distributions of the lateral swirl combustion system in DI diesel engines. Fuel. 2019; 235:1347-60. https://doi.org/10.1016/j.fuel.2018.08.133
22. Yan B, Wang H, Zheng Z, Qin Y, Yao M. The effect of combustion chamber geometry on in-cylinder flow and combustion process in a stoichiometric operation natural gas engine with EGR. Appl Therm Eng. 2018. https://doi.org/10.1016/j.applthermaleng.2017.09.067